



Original article

Antidiabetic, antioxidant, molecular docking and HPTLC analysis of miquelianin isolated from *Euphorbia schimperi* C. Presl

Sarfraz Ahmed^a, Adnan J. Al-Rehaily^a, Perwez Alam^a, Ali S. Alqahtani^a, Syed Hidayatullah^a, Md. Tabish Rehman^a, Ramzi A. Mothana^a, Syed Sadiq Abbas^b, M.U. Khan^c, Jamal M. Khalid^d, Nasir A. Siddiqui^{a,*}

^a Department of Pharmacognosy, College of Pharmacy, King Saud University, P.O. Box 2457, Riyadh 11451, Saudi Arabia

^b Department of Zoology, Shia P.G. College, Lucknow University, Lucknow, India

^c Department of Pharmaceutical Chemistry & Pharmacognosy, Unaizah College of Pharmacy, Qassim University, Al Qassim, Saudi Arabia

^d Department of Botany and Microbiology, College of Science, King Saud University, P.O. Box 2457, Riyadh 11451, Saudi Arabia

ARTICLE INFO

Article history:

Received 2 December 2018

Accepted 18 March 2019

Available online 19 March 2019

Keywords:

Miquelianin

Antidiabetic

Antioxidant

HPTLC

Quantification

ABSTRACT

The present study demonstrates the miquelianin or quercetin 3-O-glucuronide (compound **1**) isolated from aerial parts of *Euphorbia schimperi* exhibited significant results for antioxidant and antidiabetic potential. The compound **1** along with kaempferol 3-O-glucuronide (compound **2**) and quercetin 3-O-rhamnoside (compound **3**) isolated from the same source were quantified by validated HPTLC method. Antioxidant activity was determined by chemical means in terms of ABTS radical cation and DPPH radical scavenging activity. Compound **1** showed significant scavenging activity in both ABTS and DPPH assays as compared to standard BHA. In ABTS method IC₅₀ values of compound **1** and standard BHA is found to be 58.90 ± 3.40 µg/mL and 28.70 ± 5.20 µg/mL respectively while in DPPH assay IC₅₀ values of Compound **1** and standard BHA is 47.20 ± 4.90 µg/mL and 34.50 ± 6.20 µg/mL respectively. Antidiabetic effect was studied through α-amylase and α-glucosidase inhibitory activity. The mechanistic approach through molecular modelling also support the strong binding sites of compound **1** which showed significant α-amylase and α-glucosidase inhibitory activities with IC₅₀ values 128.34 ± 12.30 and 89.20 ± 9.20 µg/mL respectively as compared to acarbose 64.20 ± 5.60 and 52.40 ± 4.60 µg/mL respectively. The results of validated RP-HPTLC analyses revealed the concentration of compound **1** found to be 16.39 µg/mg and for compound **2** and compound **3** as 3.92 and 14.98 µg/mg of dried extract, respectively. © 2019 The Authors. Production and hosting by Elsevier B.V. on behalf of King Saud University. This is an open access article under the CC BY-NC-ND license (<http://creativecommons.org/licenses/by-nc-nd/4.0/>).

1. Introduction

The Euphorbiaceae is one of the largest plant family (comprising 283 genera and 7300 species) having cosmopolitan distribution in both temperate and tropical regions, of which *Euphorbia* (2000 species) is the biggest genus (Jassbi, 2006). It is well known for chemical diversity of their phytoconstituents mainly Isoprenoid type (Shi et al., 2008). The plants of *Euphorbia* produce latex con-

taining several phytoconstituents which has good therapeutic as well as commercial value. The latices of *Euphorbia* plant are unpleasant in taste and having poisonous property and protects the plant from grazing animals (AL-Sultan and Hussein, 2006). The latex also contains a number of chemical entities along with triterpene alcohol which is used as chemotaxonomic marker. Moreover, steroid, flavonoid and sesquiterpenes are also reported (Giner, 2015). *Euphorbia schimperi* C. Presl. grown in Wadi-e-Gama, Saudi Arabia (Chaudhary, 2001) apparently possess bioactivity against cancer cells, free radicals and different microorganisms (Abdel-Monem et al., 2008; Mothana et al., 2009) and also reported to contain several biologically active phytoconstituents like luteolin, α-amyrin, scopoletin, kaempferol, etc. (Abdel-Monem et al., 2008). Earlier, authors have reported that methanol extract of *E. schimperi* exhibited excellent wound healing activity (Ahmed et al., 2016) and further explored the wound healing property of its different fractions. The active fraction leads to the

* Corresponding author.

E-mail address: nsiddiqui@ksu.edu.sa (N.A. Siddiqui).

Peer review under responsibility of King Saud University.



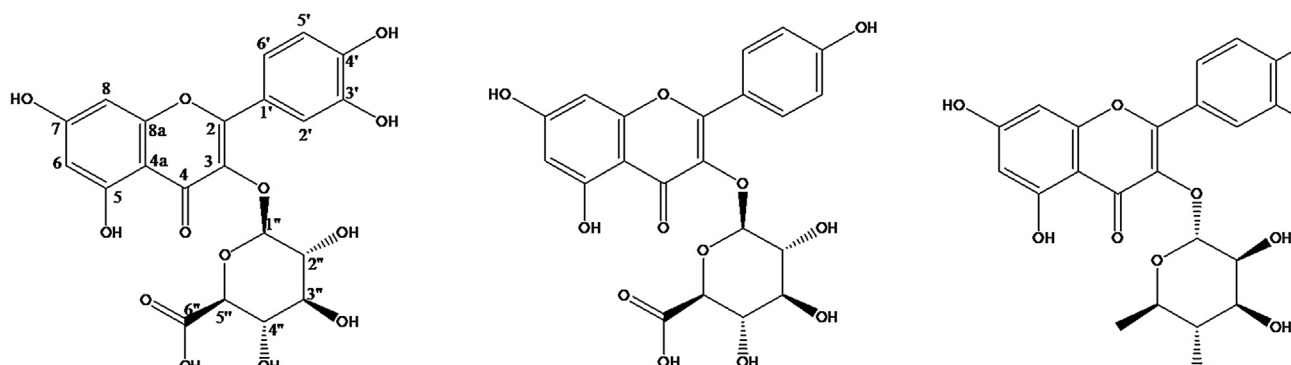


Fig. 1. Chemical structures of compounds 1–3.

isolation of a major compound quercetin-3-O-glucuronide (Compound 1) along with two minor compounds kaempferol-3-O-glucuronide (compound 2) and quercetin-3-O-rhamnoside (compound 3) (Fig. 1) using different chromatographic techniques (Ahmed et al., 2017). Kaempferol 3-O-glucuronide and quercetin-3-O-rhamnoside have also been reported from *E. guyoniana* and *E. hirta* (Smara et al., 2014; Mallavadhani et al., 2002).

Since the compounds were previously isolated from the extract having potential wound healing activity. Keeping in view present paper demonstrates the antioxidant and antidiabetic potential of natural isolate (compound 1) from *E. schimperi*. A further molecular docking study is also performed to check the reliability of antidiabetic potential. The experiments were performed because in diabetic conditions the wound healing is found to be very challenging but the natural antioxidants play a vital role in protective mechanisms by their radical scavenging and lipid peroxidation ability (Singh et al., 2014). The role of free radical reactions is well established in pathological findings particularly in various acute and chronic human ailments such as atherosclerosis diabetes, immunosuppression, neurodegeneration and aging etc. (Harman, 1998). An antioxidant can be broadly explained as any substance that inhibits or delays oxidative injury to a target molecule (Yamagishi and Matsui, 2011). The compound such as phenolic acids, polyphenols and flavonoids scavenges the free radicals like hydroperoxide and peroxide and curbing the oxidative damage caused by free radical that may lead to degenerative diseases (Wu et al.2011).

Diabetes mellitus is a metabolic disorder in which rapid rising of blood sugar level is observed. This rise in blood sugar level is either due to deficiency in making of insulin by β cells (Type 1) or somehow the produced insulin becomes inert (Type 2) (WHO, 1999). Although a lot of research has been performed to manage the diabetes and many oral hypoglycemic agents have been developed but due to certain limitations of these agents the scientific community is still trying to explore some new oral hypoglycemic agents (Kavishanker et al., 2011). Since the diabetes has been treated with medicinal plants from the ancient time, therefore the area of exploration of new antidiabetic drugs via herbs is still the field of interest and scope (Gupta et al., 2005). Various chromatographic techniques are in trend to quantify the active constituents in herbal extracts. High performance thin layer chromatography (HPTLC) is one of the reliable analytical techniques used for detection and quantification of biomarkers in plant extracts as well as marketed formulations (Siddiqui et al., 2015). Herein authors also develop a validated HPTLC method for quantification of all three compounds (1, 2 and 3) simultaneously in ESME (methanol extract of *E. schimperi*) in order to standardize the extract.

2. Experimental

2.1. Apparatus and reagents

Compounds 1, 2 and 3 (standards) were isolated from *E. schimperi* (Ahmed et al., 2017). Analytical grade reagents such as ABTS, DPPH, *p*-anisaldehyde, acarbose, α -Amylase, α -glucosidase and BHA were purchased from Sigma Aldrich. Other chemicals like dinitrosalicylic acid, sodium carbonate, *p*-nitrophenyl glucopyranoside and potassium persulphate are procured from different sources. Glass-backed silica gel 60F₂₅₄ HPTLC plates (10 × 20 cm) were purchased from Merck (Darmstadt, Germany). CAMAG automatic TLC sampler-4 (CAMAG, Muttenz, Switzerland) was used to apply the standards and samples band wise. Development was done in ADC2 (automatic development chamber), scanning in CATS 4 (CAMAG) and documentation by CAMAG TLC Reprorstar 3.

2.2. Methods

2.2.1. Antioxidant activity

2.2.1.1. ABTS radical cation scavenging activity. The ABTS [2,2'-azino-bis (3-ethylbenzothiazoline-6-sulphonic acid)] scavenging property of the compound 1 was evaluated according to the method of Re et al., 1999. Aqueous solutions of ABTS (7 mmol/L) and potassium persulfate (2.45 mmol/L) were prepared, mixed (in the ratio of 1:1) and stored in dark (for 6hrs at room temperature) to produce cation radicals. The ABTS stock solution was further diluted with ethanol and equilibrated at 30 °C ($\lambda_{max} = 734$ nm). Aliquots of compound 1 (0.1 mL) of different concentrations (20, 40, 60, 80 and 100 μ g/mL) were mixed with diluted ABTS radical cation solution (2.9 mL), incubated (at 30 °C for 20 min) and, absorbance was measured (at $\lambda = 734$ nm) using butylated hydroxyanisole (BHA) as reference compound. The ability of compound 1 to reduce the ABTS cation radicals was estimated using formula:

$$\text{Scavenging (\%)} = \left[\frac{Ac - Aa}{Ac} \right] \times 100$$

where Ac = absorbance of control; Aa = absorbance of sample.

2.2.1.2. DPPH free radical scavenging activity. The free radical scavenging property of compound 1 was assessed as per Braca et al. (2001). Aliquots of 30 μ L of various concentrations (20, 40, 60, 80 and 100 μ g/mL) of compound 1 were added in 3 mL DPPH (2,2-diphenyl-1-picrylhydrazyl) solution (0.004%) and absorbance was taken at $\lambda_{max} = 520$ nm after 30 min using Butylated hydroxyanisole (BHA) as reference and methanol as control. The free

radical scavenging ability of compound **1** was estimated as % inhibition of free radicals by following formula:

$$\% \text{ inhibition} = [(A_o - A_t)/A_o] \times 100$$

where A_t = absorbance of compound; A_o = absorbance of control.

2.2.2. Antidiabetic effect

2.2.2.1. Inhibition assay for amylase activity. The amylase inhibitory activity of compound **1** was evaluated as per [Kwon et al. \(2008\)](#). A total of 500 μL compound **1** of concentration 20, 40, 60, 80 and 100 $\mu\text{g}/\text{mL}$ and 500 μL of 0.02 M sodium phosphate buffer with 0.006 M sodium chloride, containing 20 μL of amylase (0.5 mg/mL) were incubated (at 25 °C for 10 min). Further, 1% starch solution (500 μL) in buffer (0.02 M sodium phosphate, pH 6.9 with 0.006 M sodium chloride) was added to all test tubes, incubated (for 15 min) and reaction was stopped by adding dinitrosalicylic acid (1 mL). After that all test tubes were incubated (for 5 min) in boiling water bath, cooled, diluted with distilled water (10 mL) and absorbance was measured at $\lambda_{\text{max}} = 540 \text{ nm}$.

2.2.2.2. α -Glucosidase inhibitory assay. The α -glucosidase inhibitory activity of compound **1** was evaluated as per [Kwon et al. \(2008\)](#). A 20 mM phosphate buffer (pH 6.9) was used to prepare the *p*-nitrophenyl glucopyranoside (pNPG) substrate solution. Various concentrations (20, 40, 60, 80 and 100 $\mu\text{g}/\text{mL}$) of compound **1** (50 μL) was preincubated (for 10 min.) with α -glucosidase (100 μL) and the reaction started by adding up 3.0 mM pNPG (50 μL) solution while stopped by adding 0.1 M Na_2CO_3 (2 mL) solution. The reaction mixtures were incubated (at 37 °C for 20 min) and assessed for *p*-nitrophenol release from pNPG at $\lambda_{\text{max}} = 405 \text{ nm}$. The percentage inhibition was estimated as:

$$\% \text{ Inhibition} = [(Abs_{\text{control}} - Abs_{\text{compound}})/Abs_{\text{control}}] \times 100.$$

2.2.3. Molecular docking

Autodock 4.2 was employed to perform molecular docking of compound **1** with α -amylase and α -glucosidase as described earlier ([Morris et al., 2009](#); [Rehman et al., 2016](#)). The X-ray crystal structures of α -amylase (PDB ID: 3BAW; Resolution 2.0 Å) ([Maurus et al., 2008](#)) and α -glucosidase (PDB ID: 4NN4; Resolution 1.6 Å) ([Roig-Zamboni et al., 2017](#)) were retrieved from RCSB database (<https://www.rcsb.org/>). The protein molecules were prepared by removing heterogeneous and water molecules for molecular docking. Polar hydrogen atoms and assigning Kollman charges were added by using AutoDock Tools (ADT). Affinity grid maps of $50 \times 70 \times 60 \text{ \AA}$ dimensions centered at $35 \times 30 \times 15 \text{ \AA}$ were generated for α -amylase. Similarly, for α -glucosidase, affinity grid maps of $60 \times 75 \times 70 \text{ \AA}$ dimensions centered at $20 \times -1 \times 18 \text{ \AA}$ were generated. The SDF file of compound **1** (CID: 5274585) was downloaded from NCBI database (<https://pubchem.ncbi.nlm.nih.gov/>) and converted to pdbqt using Open Babel after minimizing its energy with MMFF94 force field. The non-polar hydrogen atoms were added to the compound **1** and rotatable bonds were defined. Further, Gasteiger partial charges were added using ADT. Molecular docking was executed using Lamarck Genetic Algorithm (LGA) and Solis-Wets search procedure with default parameters. For each run of the docking, a maximum of 2.5×10^6 energy calculations was performed. The binding affinity (Kd) of compound **1** towards proteins was estimated by means of the subsequent relation ([Rehman et al., 2014](#)):

$$\Delta G = -RT \ln K_b$$

where ΔG is Gibb's free energy of interaction between protein and ligand, R is universal gas constant ($=1.987 \text{ cal/mol/K}$), and T is the experiment temperature (298°K).

2.2.4. Quantitative analysis of compounds **1**, **2** and **3** by HPTLC

2.2.4.1. HPTLC instrumentation and conditions. The HPTLC analysis of compounds **1**, **2** and **3** in ESME was performed on RP-HPTLC plates ($20 \times 10 \text{ cm}$). All the compounds along with ESME were applied on the plate by ATS-4 (Automatic TLC sampler-4; 160 nL/s) and the plate development was accomplished in Automatic Development Chamber at controlled temperature ($25 \pm 2 \text{ }^\circ\text{C}$) and humidity ($60 \pm 5\%$). The plate was dried and analyzed quantitatively (at $\lambda_{\text{max}} = 350 \text{ nm}$) in absorbance mode ([Siddiqui et al., 2018](#)).

2.2.4.2. Preparation of standard stock solutions. The stock solutions of compounds **1**, **2** and **3** (1 mg/mL) were prepared in methanol and further diluted with methanol to get seven different concentrations (20, 40, 60, 80, 100, 120 and 140 $\mu\text{g}/\text{mL}$). 10 μL of each concentration was applied on plate to provide linearity range of 200–1400 ng/spot.

2.2.4.3. Validation of method. The latest ICH Guideline for validation of analytical procedure ([ICH, 2005](#)) was adopted to determine LOD (limit of detection), LOQ (limit of quantification), linearity range, precision, robustness and recovery.

2.2.4.4. Concurrent analysis of compounds **1, **2** and **3** in ESME.** The compounds **1**, **2** and **3** were spotted on RP-HPTLC plate along with ESME and the peak areas were measured to find out its concentration ($\mu\text{g}/\text{mg}$ of dried extract) in ESME.

2.2.5. Statistical analysis

It was carried out by ANOVA (one-way analysis) and Dunnet's test for the evaluation of overall variation in a set of data. Results expressed in mean \pm SD. $P < 0.05$ considered as significant.

3. Results and discussion

3.1. Antioxidant activity

ABTS assay is frequently employed to measure the antioxidant capacities of natural products. [Fig. 2](#) shows ABTS radical scavenging activity of compound **1** and standard BHA. The compound **1** exhibited $78.00 \pm 2.80\%$ scavenging property comparable with BHA ($98.20 \pm 4.60\%$) at 100 $\mu\text{g}/\text{mL}$ concentration. The IC_{50} value ($\mu\text{g}/\text{mL}$) for compound **1** and BHA were found as 58.90 ± 3.40 and 28.70 ± 5.20 , respectively.

Compound **1** exhibited $82.90 \pm 4.30\%$ (IC_{50} : $47.20 \pm 4.90 \mu\text{g}/\text{mL}$) DPPH free radical scavenging property at 100 $\mu\text{g}/\text{mL}$ compared to

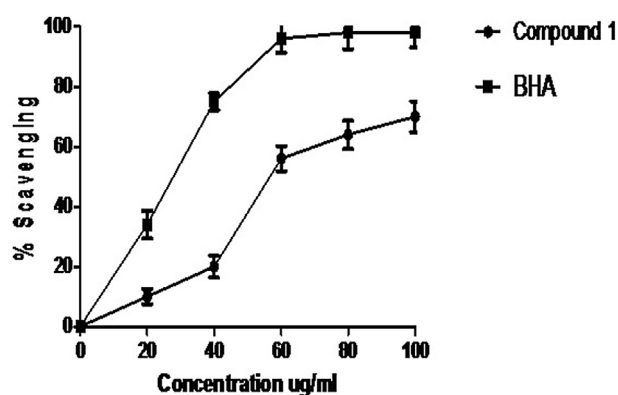


Fig. 2. ABTS scavenging activity of compound **1** and BHA. Values are means of three replicates.

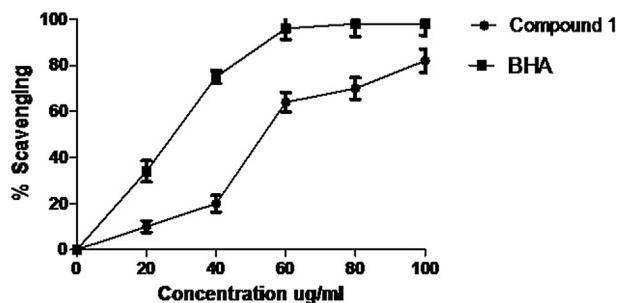


Fig. 3. DPPH scavenging activity of compound 1 and BHA. Values are means of three replicates.

BHA $93.4 \pm 1.6\%$ (IC_{50} : $34.50 \pm 6.20 \mu\text{g/mL}$) (Fig. 3). The antioxidant property of compound 1 found to increase with its increased concentration. The hydrogen or electron donated to DPPH leads to its reduction and change in its color from violet to yellow. The ability of a substance to carry out such reaction will be considered as antioxidants (Bondet et al., 1997). It is observed that several compound such as ascorbic acid, tocopherol, glutathione, pyrogallol, gallic acid and aromatic amines etc. act as hydrogen donors and decolorize 1,1 diphenyl 2 picrylhydrazyl (Blois, 1958). Several scientific reports proved the correlation between the antioxidant potential of vegetables and fruits and their total phenol contents (Deighton et al., 2000).

3.2. Antidiabetic effect

The compound 1 inhibitory property against α -amylase and α -glucosidase was evaluated and compared with acarbose. Compound 1 showed modest inhibitory effect against α -amylase (IC_{50} : $128.34 \pm 12.30 \mu\text{g/mL}$; Fig. 4) and α -glucosidase (IC_{50} : $89.20 \pm 9.20 \mu\text{g/mL}$; Fig. 5) compared to acarbose (IC_{50} : 64.20 ± 5.60 and $52.40 \pm 4.60 \mu\text{g/mL}$, respectively) given in Table 1, which is in accordance with data recently published on the inhibitory property of flavonoids against α -amylase and α -glucosidase (Kim et al., 2000). The α -Glucosidase is a renowned catalyzing enzyme used in carbohydrate digestion and glucose release. Inhibiting the action of α -glucosidase will delay the absorption of glucose and lowers the postprandial blood glucose level, which leads to the suppression and progression of Diabetes mellitus. Although, compound 1 in this experiment demonstrated average inhibitory property on both the enzymes but it required further research to clarify their potential selective α -amylase and α -glucosidase activities.

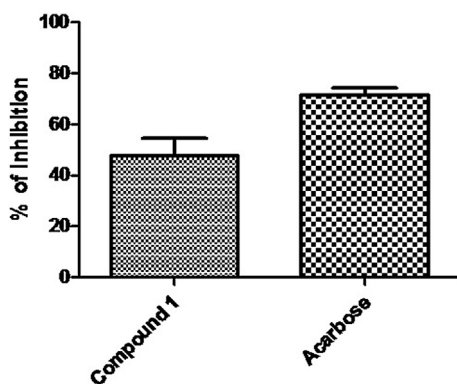


Fig. 4. IC_{50} value of compound 1 and acarbose against α amylase. Data are presented as mean \pm standard deviation values of triplicate determinations.

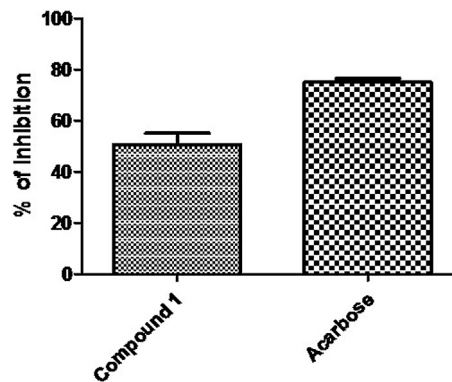


Fig. 5. IC_{50} value of compound 1 and acarbose against α glucosidase. Data are presented as mean \pm standard deviation values of triplicate determinations.

Table 1

Comparison of IC_{50} value of compound 1 and Acarbose. Values are means of three replicates \pm SD.

Sample	α -Amylase	α -Glucosidase
Compound 1	128.34 ± 12.30	89.20 ± 9.20
Acarbose	64.20 ± 5.60	52.40 ± 4.60

3.3. Molecular docking studies

AutoDock is an extensively used platform for analyzing the interaction between a protein and its ligand/inhibitor. In order to get close to the mechanism of α -amylase and α -glucosidase inhibition by compound 1, we performed molecular docking using AutoDock. We also performed molecular docking of Acarbose (an inhibitor) with α -amylase and α -glucosidase for the comparative analysis.

3.3.1. Molecular docking analysis of compound 1 with α -amylase

The results reported in Fig. 7 and Table 4 clearly revealed that compound 1 fits perfectly at the active site of α -amylase. The compound 1- α -amylase complex was stabilized by eight hydrogen bonds and three hydrophobic interactions. The amino acid residues involved in hydrogen bond formation were Trp59, Tyr62, Gln63, Arg195, Glu233, Asp300, and Gly306 (Table 2). It is very exciting to note that Asp300 formed two hydrogen bonds. Moreover, Val163 formed two hydrophobic interactions (Pi-Sigma) with compound 1 while His305 interacted with compound 1 through Pi-Pi (T-shaped) hydrophobic interaction (Fig. 6; Table 2). Other amino acid residues involved in stabilizing compound 1- α -amylase complex were Trp59, Tyr151, Leu162, Asp197, Ala198, His201, Ile235, His299, etc. The Gibbs's free energy for the interaction between compound 1 and α -amylase was estimated to be -8.2 kcal/mol , which corresponded to a binding affinity of $1.03 \times 10^6 \text{ M}^{-1}$. Similarly, Acarbose formed eight hydrogen bonds and two hydrophobic interactions with α -amylase. The amino acid residues Trp59, His101, Val163, Asp197, Glu233, and Asp300 formed only one hydrogen bond with α -amylase, while Gly104 formed two hydrogen bonds with α -amylase. On the other hand, Trp59 was involved in the formation of two hydrophobic (Pi-Alkyl) interactions with α -amylase (Fig. 7; Table 4). Other amino acid residues stabilizing the Acarbose- α -amylase were Ile49, Val50, Val51, Trp58, Glu60, Tyr62, Gln63, Gly106, Ala107, Ile162, Leu165, Ala198, His201, Ile235, His305, and Gly306. The Gibbs's free energy and binding affinity of Acarbose- α -amylase complex formation were -8.0 kcal/mol and $7.37 \times 10^5 \text{ M}^{-1}$ respectively. It is evident that the binding energy and affinity of compound 1 were comparable to a known inhibitor (Acarbose).

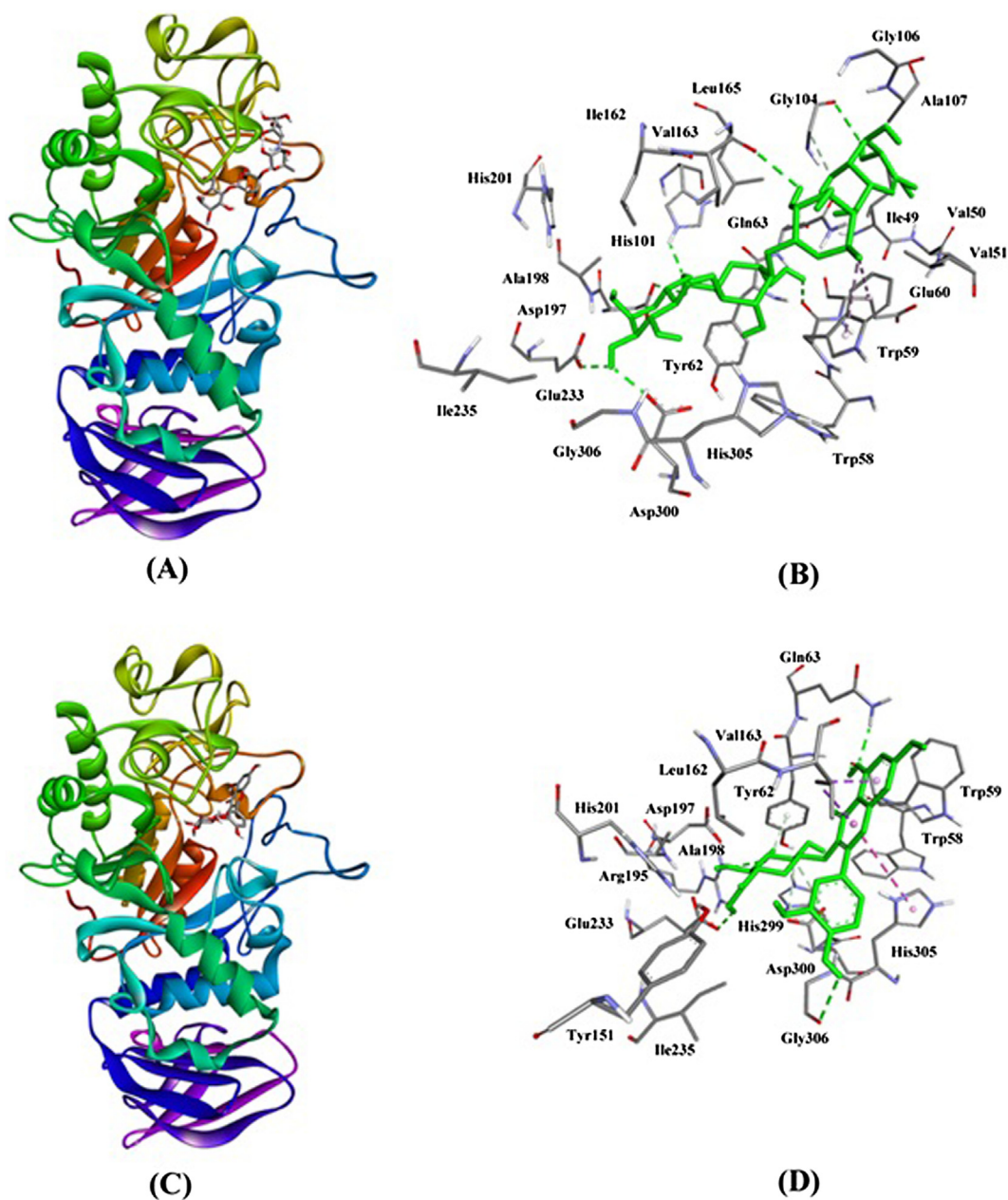


Fig. 6. Inhibition of α -amylase activity by Acarbose and compound **1**. (A) binding of Acarbose at the active site of α -amylase, (B) Interaction of Acarbose with the active site residues of α -amylase, (C) binding of compound **1** at the active site of α -amylase, and (D) Interaction of compound **1** with the active site residues of α -amylase.

The structural and mechanistic analysis of human pancreatic α -amylase revealed that it comprises three domains (A–C) (Rydberg et al., 2002). Domain A is the largest and main domain encompassing residues 1–99, and 169–404. It forms a central eight-stranded parallel β -barrel structure. At the end domain A, active site residues namely Asp197, Glu233, and Asp300 are located. A chloride ion is also bound in the vicinity of the active site and interacts with Arg195, Asn298, and Arg337. Domain B is the smallest domain of α -amylase comprising residues 100–168, and serves as the binding site of calcium ions. Domain C (residues 405–496) is mainly composed of anti-parallel β -structure, which is loosely associated with Domains A and B (Li, 2005). Our molecular docking analysis revealed that compound **1** form hydrogen bonds with two out of the three active site residues (namely Glu233 and Asp300). Moreover, it also interacted through hydrogen bonding with Arg195, one of the residue which binds with

the chloride ion (Fig. 6). These results together with the findings of *in-vitro* α -amylase activity suggest that compound **1** is a potent inhibitor of α -amylase activity.

3.3.2. Molecular docking analysis of compound **1** with α -glucosidase

The X-ray crystal structure of α -glucosidase revealed that its substrate-binding active site pocket is formed by the C-terminal ends of the catalytic GH31 or ($\beta\alpha$)₈ domain, followed by a loop from N-terminal β -sheet domain both the inserts I and II (Roig-Zamboni et al., 2017). It harbors two active site residues namely Asp518 and Asp616 which act as a catalytic nucleophile and acid/base respectively in the classical Koshland double displacement reaction mechanism. We performed molecular docking of compound **1** to evaluate its potential as an inhibitor of α -glucosidase (Fig. 7; Table 3). The results evidently suggest that compound **1** formed a hydrogen bond (2.84 Å) with OD2 of

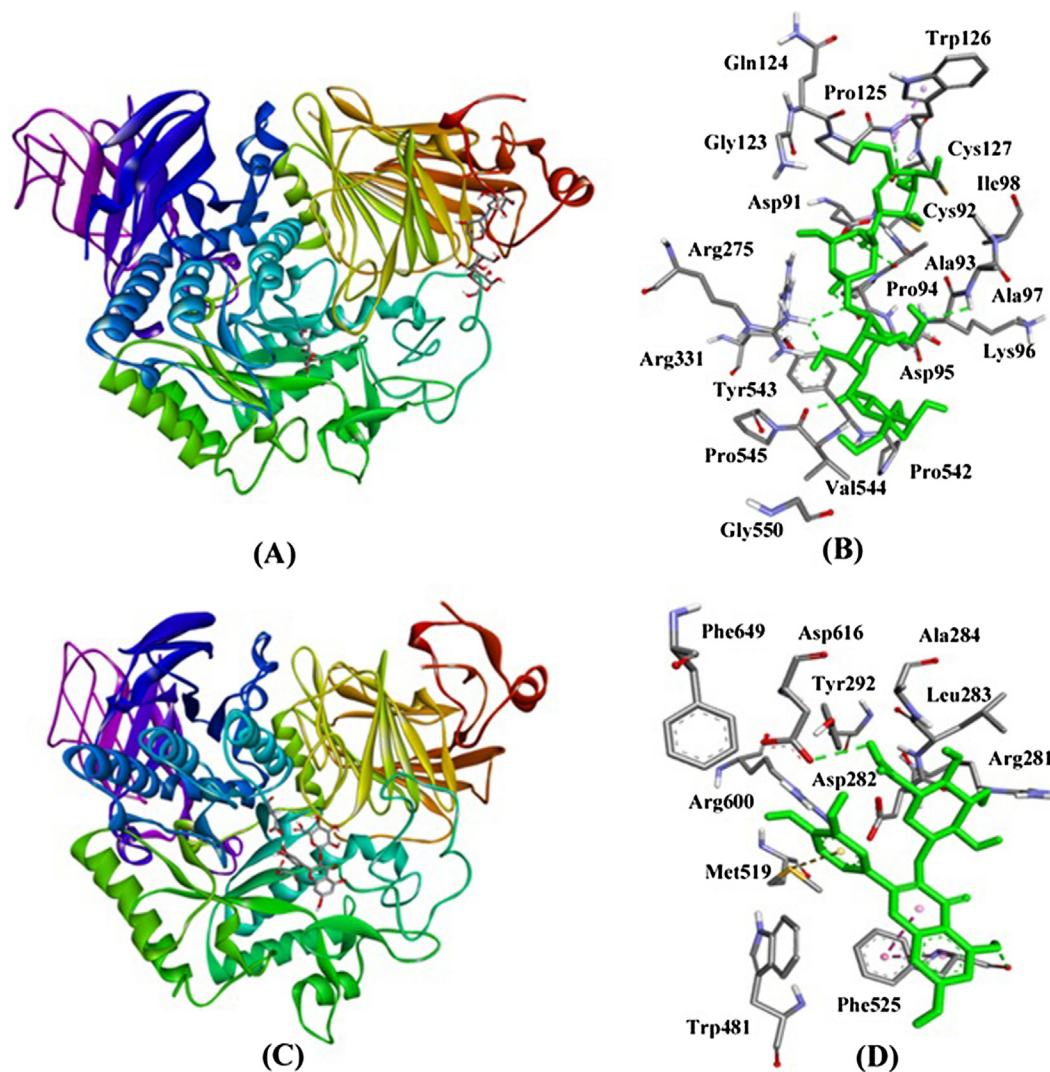


Fig. 7. Inhibition of α -glucosidase activity by Acarbose and compound **1**. (A) binding of Acarbose at Trefoil type P domain of α -glucosidase, (B) Interaction of Acarbose with the residues of α -glucosidase, (C) binding of compound **1** at the active site of α -glucosidase, and (D) Interaction of compound **1** with the active site residues of α -glucosidase.

Table 2
Inhibition of human pancreatic α -amylase by compound **1** (Miquelianin) and Acarbose.

Interacting residues	Type of interactions	Bond length (Å)	Binding free energy (ΔG), kcal/mol	Binding affinity, Kd (M^{-1})
<i>Acarbose</i>				
HIS101:HE2 – UNK:O	Hydrogen Bond	2.31	–8.0	7.37×10^5
UNK:H – GLY104:O	Hydrogen Bond	2.85		
UNK:H – VAL163:O	Hydrogen Bond	2.84		
UNK:H – TRP59:O	Hydrogen Bond	2.41		
UNK:H – GLU233:OE2	Hydrogen Bond	2.41		
UNK:H – ASP300:OD2	Hydrogen Bond	2.28		
UNK:H – ASP197:OD2	Hydrogen Bond	2.70		
GLY104:CA – UNK:O	Hydrogen Bond	3.49		
TRP59 – UNK:C	Hydrophobic (Pi-Alkyl)	5.16		
TRP59 – UNK:C	Hydrophobic (Pi-Alkyl)	4.45		
<i>Miquelianin</i>				
GLN63:HE22 – UNK:O	Hydrogen Bond	2.25	–8.2	1.03×10^6
ARG195:HH21 – UNK:O	Hydrogen Bond	2.80		
UNK:H – GLU233:OE2	Hydrogen Bond	2.29		
UNK:H – GLY306:O	Hydrogen Bond	3.09		
UNK:H – TRP59:O	Hydrogen Bond	2.62		
UNKC – ASP300:OD1	Hydrogen Bond	3.57		
UNK:C – ASP300:OD2	Hydrogen Bond	3.55		
UNK:H – TYR62	Hydrogen Bond	2.89		
VAL163:CG2 – UNK	Hydrophobic (Pi-Sigma)	3.85		
VAL163:CG2 – UNK	Hydrophobic (Pi-Sigma)	3.82		
HIS305 – UNK	Hydrophobic (Pi-Pi T-shaped)	5.82		

Table 3
Inhibition of lysosomal α -glucosidase by compound **1** (Miquelianin) and Acarbose.

Interacting residues	Type of interactions	Bond length (Å)	Binding free energy (ΔG), kcal/mol	Binding affinity, Kd (M^{-1})		
<i>Acarbose</i>						
ALA97:HN – UNK:O	Hydrogen Bond	2.80	–7.6	3.75×10^5		
TRP126:HN – UNK:O	Hydrogen Bond	2.64				
ARG275:HH12 – UNK:O	Hydrogen Bond	2.28				
ARG275:HH12 – UNK:O	Hydrogen Bond	2.13				
UNK:H – ASP91:OD2	Hydrogen Bond	2.43				
UNK:H – ALA93:O	Hydrogen Bond	2.81				
UNK:H – CYS127:O	Hydrogen Bond	2.73				
UNK:H – PRO94:O	Hydrogen Bond	2.59				
UNK:H – VAL544:O	Hydrogen Bond	1.92				
UNK:H – PRO542:O	Hydrogen Bond	2.14				
UNK:C – ASP95:O	Hydrogen Bond	3.41				
UNK:C – TRP126	Hydrophobic (Pi-Sigma)	3.87				
<i>Miquelianin</i>						
UNK:H – ASP616:OD2	Hydrogen Bond	2.84			–7.3	2.26×10^5
UNK:H – ASP282:O	Hydrogen Bond	2.29				
UNK:H – PHE525:O	Hydrogen Bond	2.33				
MET519:SD – UNK	Other (Pi-Sulphur)	5.10				
PHE525 – UNK	Hydrophobic (Pi-Pi Stacked)	3.77				
PHE525 – UNK	Hydrophobic (Pi-Pi Stacked)	3.84				

Asp616, which is an active site residue. In addition, it also formed two more hydrogen bonds with the oxygen atoms of Asp282 (2.29 Å) and Phe525 (2.33 Å). The standard 1- α -glucosidase complex was further stabilized by two hydrophobic interactions

(Pi-Pi Stacked) with Phe525 and one Pi-Sulphur interaction with the terminal Sulphur atom of Met519 (Fig. 7; Table 3). Other amino acid residues involved in the interaction were Arg281, Leu283, Ala284, Tyr292, Trp481, Arg600, and Phe649. The Gibb's free

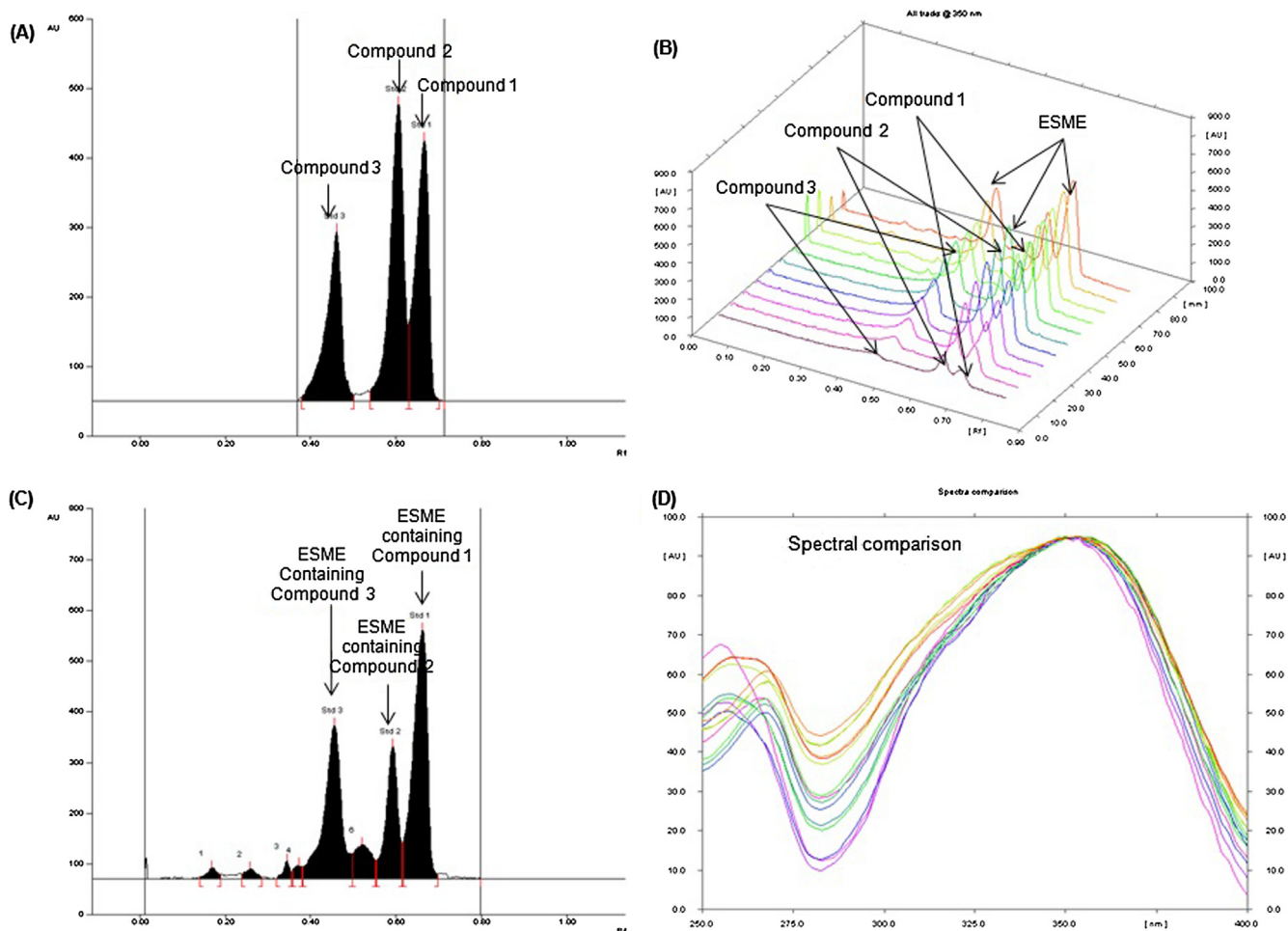


Fig. 8. Quantification of compound **1**, compound **2** and compound **3** in ESME by RP-HPTLC at $\lambda = 350$ nm [mobile phase: methanol: water (60:40)]. (A) Chromatogram of standard compound **3** ($R_f = 0.46$), compound **2** ($R_f = 0.60$) and compound **1** ($R_f = 0.66$) (B) 3-D display of all tracks (C) Chromatogram of ESME [compound **3**, spot 5, $R_f = 0.46$; compound **2**, spot 7, $R_f = 0.60$; compound **1**, spot 8, $R_f = 0.66$]. (D) Spectral comparison of all the tracks at 350 nm.

Table 4
R_f, Linear regression data for the calibration curve of compound **1**, compound **2** and compound **3** (n = 6).

Parameters	Compound 1	Compound 2	Compound 3
Linearity range (ng/spot)	200–1400	200–1400	200–1400
Regression equation	Y = 7.517X + 518.11	Y = 7.593X + 2193.06	Y = 4.822X + 221.71
Correlation (r ²) coefficient	0.9964 ± 0.001	0.9942 ± 0.002	0.9972 ± 0.001
Slope ± SD	7.517 ± 0.016	7.593 ± 0.035	4.822 ± 0.048
Intercept ± SD	518.11 ± 9.18	2193.06 ± 45.91	221.71 ± 16.15
Standard error of slope	0.006	0.014	0.019
Standard error of intercept	3.74	18.73	6.592
R _f	0.66 ± 0.002	0.60 ± 0.003	0.46 ± 0.003
LOD (ng)	7.42	15.51	33.21
LOQ (ng)	22.43	47.01	100.66

energy (ΔG) of interaction between compound **1** and α -glucosidase was estimated to be -7.3 kcal/mol, corresponding to a binding affinity (Kd) of 2.26×10^5 M⁻¹. Recently, Roig-Zamboni et al., 2017) also confirmed that 1-deoxynojirimycin (a well-establish inhibitor of α -glucosidase) binds at the active site of α -glucosidase and interacts with Trp376, Asp404, Ile441, Trp516, Asp518, Met519, Arg600, Trp613 Asp616, Phe649, and His674 through multiple hydrogen bonds and hydrophobic interactions. Conversely, Acarbose binds at the Trefoil type P domain of α -glucosidase and the complex was stabilized by eleven hydrogen bonds (with Asp91, Ala93, Pro94, Asp95, Ala97, Trp126, Cys127, Arg275, Pro542, and Val544) and one hydrophobic interaction with Trp126 (Fig. 7). It should be noted that Arg275 formed two hydrogen bonds with the Oxygen atoms of α -glucosidase. The Gibb's free energy (ΔG) and binding affinity (Kd) for the standard 1- α -glucosidase complex formation were estimated to be -7.6 kcal/mol, and 3.75×10^5 M⁻¹ respectively. From these results, we infer that the binding sites of Acarbose and compound **1** on α -glucosidase were different but they both interact with the key residues of α -glucosidase and act as an inhibitor.

3.4. HPTLC method development and validation

The mobile phase for the HPTLC investigation of compounds **1**, **2** and **3** in ESME was selected by trying combinations of different solvents. Of these a mixture of methanol and water (60:40, v/v) was found suitable to furnish sharp, compact and intense peak of compounds **1**, **2** and **3** (at R_f = 0.66 ± 0.002, 0.60 ± 0.003 and 0.46 ± 0.003, respectively; Fig. 8A). This method clearly separated the compounds **1**, **2** and **3** in addition to the constituents of ESME (Fig. 8B). The above method was fairly selective with high baseline resolution. The peaks of standard and the extracts were compared by aligning each other at wavelength 350 nm (Fig. 8D). The regression equation/correlation co-efficient (r²) for compounds **1**, **2** and **3** were obtained as Y = 7.517X + 518.11/0.9964, Y = 7.593X + 2193.06/0.9942 and Y = 4.822X + 221.71/0.9972, respectively in 200–1400 ng/spot linearity range. The LOD/ LOQ (ng/band) for compounds **1**, **2** and **3** were calculated as 7.42/22.43, 15.51/47.01 and 33.21/100.66 ng/band, respectively (Table 4). The recoveries as accuracy study of above method were calculated and reported in Table S1 (Table attached as suppl. material). The (%) recovery/RSD for compounds **1**, **2** and **3** were found as 98.21–99.41/1.05–1.19, 98.71–99.54/ 1.37–1.44 and 98.72–99.39/1.27–1.33, respectively. The intra-day/ inter-day precision (% RSD; n = 6) of the above method for the compounds **1**, **2** and **3** were calculated and recorded as 1.17–1.24/ 1.09–1.22, 1.32–1.37/1.31–1.35 and 1.04–1.12/1.03–1.10, respectively and recorded in Table S2 (Table attached as suppl. material) which demonstrated good precision of proposed method. The robustness for the above method

Table 5
HPTLC analysis of compound **1**, compound **2** and compound **3** in ESME.

S. No.	Sample	Compound 1 content (μg/mg of dried weight of extract)	Compound 2 content (μg/mg of dried weight of extract)	Compound 3 content (μg/mg of dried weight of extract)
1	ESME	16.39 ± 0.89	3.92 ± 0.019	14.98 ± 0.79

was tested by creating a small intentional change in composition of mobile phase, saturation time and volume of mobile phase used and the obtained data were reported in Table S3 (attached as suppl. material). The low SD and % RSD indicated that above method was robust.

3.5. Concurrent HPTLC analysis of compounds **1**, **2** and **3** in ESME

The selected HPTLC method was used for concurrent analysis of compounds **1**, **2** and **3** in the ESME (Fig. 8C). Using the above method the quantity of compounds **1**, **2** and **3** was found as 16.39, 3.92 and 14.98 μg/mg of dried extract, respectively (Table 5).

The results of HPTLC analysis of Compound **1** (miquelianin; 16.39 μg/mg) strongly support the therapeutic uses of *E. schimperi*. Quantification of compound **2** (kaempferol 3-O-glucuronide) and compound **3** (quercetin 3-O-rhamnoside) in methanol extract of *E. schimperi* provides additional information about their quantity which will facilitate the formulation designing.

4. Conclusion

The study revealed significant antidiabetic and antioxidant property of miquelianin which is strongly aligned with its molecular docking results, and approves our previous work on wound healing. This was a maiden study on the concurrent HPTLC analysis of miquelianin, kaempferol-3-O-glucuronide and quercetin-3-O-rhamnoside in ESME. The chromatographic quantification proves the ample amount of miquelianin present in ESME which offers the medicinal use of extract as such or as a component in a poly herbal formulation. The proposed HPTLC method can be applied in the investigation of miquelianin, kaempferol 3-O-glucuronide and quercetin 3-O-rhamnoside in other plant species extracts and marketed herbal preparations.

Acknowledgement

The authors extend their appreciation to the Deanship of Scientific Research at King Saud University, Riyadh, Saudi Arabia for funding the work through the research group project number (RGP - 073).

Appendix A. Supplementary material

Supplementary data to this article can be found online at <https://doi.org/10.1016/j.sjps.2019.03.008>.

References

- Abdel-Monem, A.R., Abdel-Sattar, E., Harraz, F.M., Petereit, F., 2008. Chemical investigation of *Euphorbia schimperi* C. Presl. Rec. Nat. Prod. 2, 39–45.
- Ahmed, S., Nur-e-alam, M., Mothana, R.A., Yousaf, M., Al-Rehaily, A.J., 2017. Activity guided isolation of chemical constituents from the biologically active methanol extract of *Euphorbia schimperi* c. presl. Bull. Chem. Soc. Ethiop. 31, 471–479.
- Ahmed, S., Yousaf, M., Mothana, R.A., Al-Rehaily, A.J., 2016. Studies on wound healing activity of some *Euphorbia* species on experimental rats. Afr. J. Tradit. Complement. Altern. Med. 13, 45–52.
- Al-Sultan, S.I., Hussein, Y.A., 2006. Acute toxicity of *Euphorbia helioscopia* in Rats. Pak. J. Nut. 5, 135–140.
- Blois, M.S., 1958. Antioxidant determinations by the use of a stable free radical. Nature 29, 1199–1200.
- Bondet, V., Brand-Williams, W., Berset, C., 1997. Kinetics and mechanisms of antioxidant activity using the DPPH free radical method. Lebensm.-Wiss. u. Technol. 30, 609–615.
- Braca, A., De Tommasi, N., Di Bari, L., Pizzi, C., Politi, M., Morelli, I., 2001. Antioxidant principles from *Bauhinia tarapotensis*. J. Nat. Prod. 64, 892–895.
- Chaudhary, S.A., 2001. Flora of Kingdom of Saudi Arabia I Illustrated. Ministry of Agriculture and Water, National Herbarium, National Agriculture and Water Research Center, Riyadh.
- Deighton, N., Brennan, R., Finn, C., Davies, H.V., 2000. Antioxidant properties of domesticated and wild *Rubus species*. J. Sci. Food Agric. 80, 1307–1313.
- Giner, J.L., Schroeder, T.N., 2015. Polygonifoliol, a new tirucallane triterpene from the latex of the seaside sandmat *Euphorbia polygonifolia*. Chem. Biodivers. 12, 1126–1129.
- Gupta, R.K., Kesari, A.N., Murthy, P.S., Chandra, R., Tandon, V., Watal, G., 2005. Hypoglycemic and anti-diabetic effect of ethanolic extract of leaves of *Annona squamosa* L. in experimental animals. J. Ethnopharmacol. 99, 75–81.
- Harman, D., 1998. Free Radical Theory of Aging. Current Status. Elsevier, Amsterdam, pp. 3–7.
- International Conference on Harmonization (ICH) of Technical Requirements for Registration of Pharmaceuticals for Human use, Harmonised Tripartite Guideline on Validation of Analytical Procedures: Text and Methodology Q2 (R1), Complementary Guideline on Methodology incorporated in November 2005 by the ICH Steering Committee, IFPMA, Geneva.
- Jassbi, A.R., 2006. Chemistry and biological activity of secondary metabolites in *Euphorbia* from Iran. Phytochemistry 67, 1977–1984.
- Kavishankar, G.B., Lakshmidevi, N., Murthy, S.M., Prakash, H.S., Niranjana, S.R., 2011. Diabetes and medicinal plants: a review. Int. J. Pharm. Biomed. Sci. 2, 65–80.
- Kim, J.S., Kwon, C.S., Son, K.H., 2000. Inhibition of alpha-glucosidase and amylase by luteolin, a flavonoid. Biosci. Biotechnol. Biochem. 64, 2458–2461.
- Kwon, Young-In, Apostolidis, E., Shetty, K., 2008. Inhibitory potential of wine and tea against α -amylase and α -glucosidase for management of hyperglycemia linked to type 2 diabetes. J. Food Biochem. 32, 15–31.
- Mallavadhani, U.V., Sahu, G., Narasimhan, K., Muralidhar, J., 2002. Quantitative estimation of an antidiarrhoeic marker in *euphorbia hirta* samples. Pharmaceut. Bio. 40, 103–106.
- Maurus, R., Begum, A., Williams, L.K., Fredriksen, J.R., Zhang, R., Withers, S.G., Brayer, G.D., 2008. Alternative catalytic anions differentially modulate human alpha-amylase activity and specificity. Biochemistry 47, 3332–3344.
- Morris, G.M., Huey, R., Lindstrom, W., Sanner, M.F., Belew, R.K., Goodsell, D.S., Olson, A.J., 2009. Autodock4 and AutoDockTools4: automated docking with selective receptor flexibility. J. Comput. Chem. 16, 2785–2791.
- Mothana, R.A., Gruenert, R., Bednarski, P.J., Lindequist, U., 2009. Evaluation of the in vitro anticancer, antimicrobial and antioxidant activities of some Yemeni plants used in folk medicine. Die Pharmazie. 64, 260–268.
- Re, R., Pellegrini, N., Proteggente, A., Pannala, A., Yang, M., Rice-Evans, C., 1999. Antioxidant activity applying an improved ABTS radical cation decolorization assay. Free Radic. Biol. Med. 26, 1231–1237.
- Rehman, M.T., Ahmed, S., Khan, A.U., 2016. Interaction of meropenem with 'N' and 'B' isoforms of human serum albumin: a spectroscopic and molecular docking study. J. Biomol. Struct. Dyn. 34, 1849–1864.
- Rehman, M.T., Shamsi, H., Khan, A.U., 2014. Insight into the binding mechanism of imipenem to human serum albumin by spectroscopic and computational approaches. Mol. Pharmaceut. 11, 1785–1797.
- Roig-Zamboni, V.R., Cobucci-Ponzano, B., Iacono, R., Ferrara, M.C., Germany, S., Bourne, Y., Parenti, G., Moracci, M., Sulzenbacher, G., 2017. Structure of human lysosomal acid α -glucosidase – a guide for the treatment of Pompe disease. Nat. Commun. 8, 1111.
- Rydberg, E.H., Li, C., Maurus, R., Overall, C.M., Brayer, G.D., Withers, S.G., 2002. Mechanistic analyses of catalysis in human pancreatic alpha-amylase: detailed kinetic and structural studies of mutants of three conserved carboxylic acids. Biochemistry 41, 4492–4502.
- Shi, Q.W., Su, X.H., Kiyota, H., 2008. Chemical and pharmacological research of the plants in genus *Euphorbia*. Chem. Rev. 108, 4295–4327.
- Singh, A., Singh, P.K., Singh, R.K., 2014. Antidiabetic and wound healing activity of *catharanthus roseus* l. in streptozotocin-induced diabetic mice. Am. J. Phytomed. Clin. Therapeut. 2, 686–692.
- Siddiqui, N.A., Alam, P., Al-Rehaily, A.J., Al-Oqail, M.M., Parvez, M.K., 2015. Simultaneous quantification of biomarkers bergenin and menisdaurin in the methanol extract of aerial parts of *Flueggea virosa* by validated HPTLC densitometric method. J. Chromatogr. Sci. 53 (5), 824–829.
- Siddiqui, N.A., Al-Yousef, H.M., Alhowiriny, T.A., Alam, P., Hassan, W.H.B., Musarat, A., Hussain, A., Abdelaziz, S., Abdallah, R.H., 2018. Concurrent analysis of bioactive triterpenes oleanolic acid and b-amyirin in antioxidant active fractions of *Hibiscus calyphyllus*, *Hibiscus deflersii* and *Hibiscus micranthus* grown in Saudi Arabia by applying validated HPTLC method. Saudi Pharmaceut. J. 26, 266–273.
- Smara, O., Julia, A., Moral-Salmi, C., Vigor, C., Joseph, V., Legseir, B., 2014. Flavonoids from *Euphorbia guyoniana* Boissier & Reuter. J. Life Sci. 8, 544–551.
- WHO, 1999. Expert Committee on Diabetes Mellitus: Diagnosis and Classification of Diabetes Mellitus Technical Report Series. Part 1. World Health Organization, Geneva.
- Wu, Y.Y., Li, W., Xu, Y., Jin, E.H., Tu, Y.Y., 2011. Evaluation of the antioxidant effects of four main theaflavin derivatives through chemiluminescence and DNA damage analyses. J. Zhejiang Univ. Sci. B 12, 744–751.
- Yamagishi, S., Matsui, T., 2011. Nitric oxide, a Janus-faced therapeutic target for diabetic microangiopathy-friend or foe? Pharmacol. Res. 64, 187–194.